ForestTemp – Sub-canopy microclimate temperatures of European forests

Journal Article

Author(s):
Haesen, Stef; Lembrechts, Jonas J.; De Frenne, Pieter; Lenoir, Jonathan; Aalto, Juha; Ashcroft, Michael B.; Kopecky, Martin; Luoto, Miska; Maclean, Ilya; Nijs, Ivan; Niittynen, Pekka; van den Hoogen, Johan (iD); Arriga, Nicola; Bruna, Josef; Buchmann, Nina (iD); Čiliak, Marek; Collalti, Alessio; De Lombaerde, Emiel; Descombes, Patrice (iD); Gharun, Mana; Shekhar, Ankit (iD); et al.

ForestTemp – sub-canopy microclimate temperatures of European forests

Journal:	*Global Change Biology*
Manuscript ID	GCB-21-0917.R1
Wiley - Manuscript type:	Technical Advances
Date Submitted by the Author:	n/a
Complete List of Authors:	Haesen, Stef; KU Leuven, Department of Earth and Environmental Sciences Lembrechts, Jonas; University of Antwerp De Frenne, Pieter; Ghent University, Forest & Nature Lab Lenoir, Jonathan; Université de Picardie Jules Verne, Plant Biodiversity Lab (EA 4698) Aalto, Juha; Finnish Meteorological Institute Ashcroft, Michael; University of Wollongong, School of Biological Sciences Kopecký, Martin; Czech Academy of Sciences, Department of Vegetation Ecology, Institute of Botany Luoto, Miska; University of Helsinki, Department of Geosciences and Geography Maclean, Ilya M D; Centre for Ecology and Conservation, School of Biosciences Nijs, Ivan; University of Antwerp, Research Group of Plant and Vegetation Ecology, Department of Biology Niittynen, Pekka; Helsingin Yliopisto, Department of Geosciences and Geography van den Hoogen, Johan; ETH Zurich Department of Environmental Systems Science Arriga, Nicola; European Commission Joint Research Centre Ispra Sector Bruna, Josef; The Czech Academy of Sciences, Institute of Botany Buchmann, Nina; ETH Zürich, Institute of Agricultural Sciences Ciliak, Marek; Technical University of Zvolen Collalti, Alessio; Euro-Mediterranean Center on Climate Change, IAFES; National Research Council of Italy, ISAFOM De Lombaerde, Emiel; Ghent University Descombes, Patrice; Swiss Federal Institute for Forest, Snow and Landscape Research, Gharun, Mana; ETH Zurich Department of Environmental Systems Science, ; ETH Zürich Goded, Ignacio; European Commission Joint Research Centre Ispra Sector Govaert, Sanne; Ghent University Faculty of Bioscience Engineering, Environment Greiser, Caroline; Stockholm University Grelle , Achim; Swedish University of Agricultural Sciences Gruening, Carsten; European Commission Joint Research Centre

Hederová, Lucia; Institute of Botany Czech Academy of Sciences
Hylander, Kristoffer; Stockholm University, Department of Ecology, Environment and Plant Sciences
Kreyling, Juergen; Ernst-Moritz-Arndt Universitat Greifswald, Experimental Plant Ecology
Kruijt, Bart; Wageningen University & Research
Macek, Martin; Institute of Botany Czech Academy of Sciences,
Máliš, František; Technical University in Zvolen, Department of Phytology, Faculty of Forestry
Man, Matěj; Institute of Botany Czech Academy of Sciences
Manca, Giovanni; European Commission Joint Research Centre Ispra Sector
Matula, Radim; Czech University of Life Sciences Prague
Meeussen, Camille; Ghent University, Environment
Merinero, Sonia; Stockholm University, Department of Ecology, Environment and Plant Sciences and Bolin Centre for Climate Research; University of Seville, Department of Plant Biology and Ecology
Minerbi, Stefano; Provincia Autonoma di Bolzano Servizi Forestali
Montagnani, Leonardo; Forest Services, ; Libera Universita di Bolzano, Faculty of Science and Technology
Muffler, Lena; University of Gottingen Albrecht-von-Haller-Institute for Plant Sciences, Plant Ecology; University Greifswald Institute of Botany and Landscape Ecology, Experimental Plant Ecology
Ogaya, Romà; CREAF-CSIC, Ecophysiology
Penuelas, Josep; CREAF-CSIC , Global Ecology
Plichta, Roman; Mendel University in Brno
Portillo-Estrada, Miguel; University of Antwerp, Department of Biology
Schmeddes, Jonas; Ernst-Moritz-Arndt Universitat Greifswald
Shekhar, Ankit; ETH Zürich, D-USYS
Spicher, Fabien; Université de Picardie Jules Verne, Plant Biodiversity Lab (EA 4698)
Ujházyová, Mariana; Technical University of Zvolen
Vangansbeke, Pieter; Ghent University, Forest & Nature Lab
Weigel, Robert; University of Gottingen
Wild, Jan; Institute of Botany, Průhonice, Czech Republic,
Zellweger, Florian; Swiss Federal Research Institute WSL
Van Meerbeek, Koenraad; KU Leuven, Department of Earth and Environmental Sciences

Abstract:

Ecological research heavily relies on coarse-gridded climate data based on standardised temperature measurements recorded at 2 m height in open landscapes. However, many organisms experience environmental conditions that differ substantially from those captured by these macroclimatic (i.e. free-air) temperature grids. In forests, the tree canopy functions as a thermal insulator, and buffers sub-canopy microclimatic conditions, thereby affecting biological and ecological processes. To improve the assessment of climatic conditions and climate change-related impacts on forest-floor biodiversity and functioning, temperature grids reflecting forest microclimates are thus urgently needed. Combining more than 1,200 time series of in situ near-surface forest temperatures with topographical, biological and macroclimatic variables in a machine learning model, we predicted the mean monthly offset between sub-canopy temperature at 15 cm above the surface and free-air temperature over the period 2000-2020 at a spatial resolution of 25 m across Europe. This offset was used to evaluate the difference between micro- and macroclimate across space and seasons and finally enabled us to calculate mean annual and monthly temperatures for European forest understories. We found that sub-canopy air

| | temperatures differ substantially from free-air temperatures, being on average 2.1°C (standard deviation ± 1.6°C) lower in summer and 2.0°C higher (± 0.7°C) in winter across Europe. Additionally, our high-resolution maps expose considerable microclimatic variation within landscapes, not captured by the gridded macroclimatic products. The provided forest sub-canopy temperature maps will enable future research to more accurately model below-canopy biological processes and patterns, as well as species distributions. |
| | |

SCHOLARONE™
Manuscripts

1　**ForestTemp – sub-canopy microclimate temperatures of European forests**

2　Running title – 25m-grids of sub-canopy temperature

3　*Stef Haesen[1], Jonas J. Lembrechts[2], Pieter De Frenne[3], Jonathan Lenoir[4], Juha Aalto[5], Michael B.*

4　*Ashcroft[6], Martin Kopecký[7,8], Miska Luoto[9], Ilya Maclean[10], Ivan Nijs[2], Pekka Niittynen[9], Johan van*

5　*den Hoogen[11], Nicola Arriga[12], Josef Brůna[7], Nina Buchmann[11], Marek Čiliak[13], Alessio Collalti[14],*

6　*Emiel De Lombaerde[3], Patrice Descombes[15,16], Mana Gharun[11], Ignacio Goded[12], Sanne Govaert[3],*

7　*Caroline Greiser[17], Achim Grelle[18], Carsten Gruening[12], Lucia Hederová[7], Kristoffer Hylander[17], Jürgen*

8　*Kreyling[19], Bart Kruijt[20], Martin Macek[7], František Máliš[21], Matěj Man[7], Giovanni Manca[12], Radim*

9　*Matula[8], Camille Meeussen[3], Sonia Merinero[17,22], Stefano Minerbi[23], Leonardo Montagnani[23,24], Lena*

10　*Muffler[25], Romà Ogaya[26], Josep Penuelas[26,27], Roman Plichta[28], Miguel Portillo-Estrada[2], Jonas*

11　*Schmeddes[19], Ankit Shekhar[11], Fabien Spicher[4], Mariana Ujházyová[13], Pieter Vangansbeke[3], Robert*

12　*Weigel[25], Jan Wild[7], Florian Zellweger[29], Koenraad Van Meerbeek[1]*

13　*Corresponding author, OrcID = https://orcid.org/0000-0002-4491-4213, stef.haesen@kuleuven.be,*

14　*+32 16 32 24 67*

15　*[1]Department of Earth and Environmental Sciences, Celestijnenlaan 200E, 3001 Leuven, Belgium;*

16　*[2]Research Group PLECO (Plants and Ecosystems), University of Antwerp, 2610 Wilrijk, Belgium; [3]Forest*

17　*& Nature Lab, Department of Environment, Ghent University, Geraardsbergsesteenweg 267, 9090*

18　*Melle-Gontrode, Belgium; ; [4]UMR CNRS 7058 'Ecologie et Dynamique des Systèmes Anthropisés'*

19　*(EDYSAN), Univ. de Picardie Jules Verne, Amiens, France; [5]Finnish Meteorological Inst., P.O. Box 503,*

20　*FI-00101 Helsinki, Finland; [6]Centre for Sustainable Ecosystem Solutions, School of Biological Sciences,*

21　*University of Wollongong, Wollongong, Australia; [7]Institute of Botany of the Czech Academy of*

22　*Sciences, Zámek 1, CZ-25243, Průhonice, Czech Republic; [8]Faculty of Forestry and Wood Sciences, Czech*

23　*University of Life Sciences Prague, Kamýcká 129, CZ-165 21, Prague 6 - Suchdol, Czech Republic; [9]Dept*

24　*of Geosciences and Geography, Gustaf Hällströmin katu 2a, FIN–00014 Univ. of Helsinki, Finland;*

25　*[10]Environment and Sustainability Institute, University of Exeter, Penryn Campus, Penryn, UK, TR10 9FE;*

26　*[11]Department of Environmental Systems Science, ETH Zurich, Universitaetstrasse 2, 8092 Zurich,*

27　*Switzerland; [12]European Commission, Joint Research Centre (JRC), Ispra, Italy; [13]Faculty of Ecology and*

28　*Environmental Sciences, Technical University in Zvolen, T.G.Masaryka 24, 960 01 Zvolen, Slovakia;*

29　*[14]Institute for Agriculture and Forestry Systems in the Mediterranean, National Research Council of*

30　*Italy (CNR-ISAFOM), Perugia, Italy; [15]Dept. of Ecology & Evolution, University of Lausanne, 1015*

31　*Lausanne, Switzerland; [16]Musée et Jardins botaniques Cantonaux, 1007 Lausanne, Switzerland;*

32　*[17]Department of Ecology, Environment and Plant Sciences and Bolin Centre for Climate Research,*

33　*Stockholm University, 106 91 Stockholm, Sweden; [18]Department of Ecology, Swedish University of*

Agricultural Sciences, Uppsala, Sweden; [19]Experimental Plant Ecology, Institute of Botany and

Landscape Ecology, University of Greifswald, D-17487 Greifswald, Germany; [20]Wageningen University

and Research, Wageningen, Netherlands; [21]Faculty of Forestry, Technical University in Zvolen,

T.G.Masaryka 24, 960 01 Zvolen, Slovakia; [22]Department of Plant Biology and Ecology, University of

Seville, Apartado 1095, 41080 Seville, Spain; [23]Forest Services, Autonomous Province of Bolzan, 39100

Bolzano, Italy; [24]Faculty of Science and Technology, Free University of Bolzano, 39100 Bolzano, Italy;

[25]Plant Ecology, Albrecht-von-Haller-Institute for Plant Sciences, Georg-August University of

Goettingen, Untere Karspuele 2, 37073 Goettingen, Germany; [26]CSIC, Global Ecology Unit CREAF- CSIC-

UAB, Bellaterra, 08193, Catalonia, Spain; [27]CREAF, Cerdanyola del Vallès 08193, Catalonia, Spain;

[28]Department of Forest Botany, Dendrology and Geobiocoenology, Mendel University in Brno, Czech

Republic; [29]Swiss Federal Institute for Forest, Snow and Landscape Research WSL, Birmensdorf,

Switzerland

OrcIDs

Jonas J. Lembrechts: https://orcid.org/0000-0002-1933-0750

Pieter De Frenne: https://orcid.org/0000-0002-8613-0943

Juha Aalto: https://orcid.org/0000-0001-6819-4911

Martin Kopecký: https://orcid.org/0000-0002-1018-9316

Jonathan Lenoir: https://orcid.org/0000-0003-0638-9582

Miska Luoto: https://orcid.org/0000-0001-6203-5143

Ilya Maclean: https://orcid.org/0000-0001-8030-9136

Ivan Nijs: https://orcid.org/0000-0003-3111-680X

Pekka Niittynen: https://orcid.org/0000-0002-7290-029X

Johan van den Hoogen: https://orcid.org/0000-0001-6624-8461

Nicola Arriga: https://orcid.org/0000-0001-5321-3497

Josef Brůna: https://orcid.org/0000-0002-4839-4593

Nina Buchmann: https://orcid.org/0000-0003-0826-2980

Marek Čiliak: https://orcid.org/0000-0002-6720-9365

Alessio Collalti: https://orcid.org/0000-0002-4980-8487

Emiel De Lombaerde: https://orcid.org/0000-0002-0050-2735

Patrice Descombes: https://orcid.org/0000-0002-3760-9907

Mana Gharun: https://orcid.org/0000-0003-0337-7367

Ignacio Goded: https://orcid.org/0000-0002-1912-325X

Sanne Govaert: https://orcid.org/0000-0002-8939-1305

Caroline Greiser: https://orcid.org/0000-0003-4023-4402

Achim Grelle: https://orcid.org/0000-0003-3468-9419

Carsten Gruening: https://orcid.org/0000-0002-6169-2827

Lucia Hederová: https://orcid.org/0000-0003-1283-0952

Kristoffer Hylander: https://orcid.org/0000-0002-1215-2648

Jürgen Kreyling: https://orcid.org/0000-0001-8489-7289

Bart Kruijt: https://orcid.org/0000-0002-6186-1731

Martin Macek: https://orcid.org/0000-0002-5609-5921

František Máliš: https://orcid.org/0000-0003-2760-6988

Matěj Man: https://orcid.org/0000-0002-4557-8768

Giovanni Manca: https://orcid.org/0000-0002-9376-0310

Radim Matula: https://orcid.org/0000-0002-7460-0100

Camille Meeussen: https://orcid.org/0000-0002-5869-4936

Sonia Merinero: https://orcid.org/0000-0002-1405-6254

Stefano Minerbi: https://orcid.org/0000-0002-6620-2735

Leonardo Montagnani: https://orcid.org/0000-0003-2957-9071

Lena Muffler: https://orcid.org/0000-0001-8227-7297

Romà Ogaya: http://orcid.org/0000-0003-4927-8479

Josep Penuelas: https://orcid.org/0000-0002-7215-0150

Roman Plichta: https://orcid.org/0000-0003-2442-8522

Miguel Portillo-Estrada: https://orcid.org/0000-0002-0348-7446

Ankit Shekhar: https://orcid.org/0000-0003-0802-2821

Fabien Spicher: https://orcid.org/0000-0002-9999-955X

Mariana Ujházyová: https://orcid.org/0000-0002-5546-1547

Pieter Vangansbeke: https://orcid.org/0000-0002-6356-2858

Robert Weigel: https://orcid.org/0000-0001-9685-6783

Wild Jan: https://orcid.org/0000-0003-3007-4070

Florian Zellweger: https://orcid.org/0000-0003-1265-9147

Koenraad Van Meerbeek: https://orcid.org/0000-0002-9260-3815

72   **ABSTRACT**

73   Ecological research heavily relies on coarse-gridded climate data based on standardised temperature

74   measurements recorded at 2 m height in open landscapes. However, many organisms experience

75   environmental conditions that differ substantially from those captured by these macroclimatic (i.e.

76   free-air) temperature grids. In forests, the tree canopy functions as a thermal insulator, and buffers

77   sub-canopy microclimatic conditions, thereby affecting biological and ecological processes. To

78   improve the assessment of climatic conditions and climate change-related impacts on forest-floor

79   biodiversity and functioning, temperature grids reflecting forest microclimates are thus urgently

80   needed. Combining more than 1,200 time series of *in situ* near-surface forest temperatures with

81   topographical, biological and macroclimatic variables in a machine learning model, we predicted the

82   mean monthly offset between sub-canopy temperature at 15 cm above the surface and free-air

83   temperature over the period 2000-2020 at a spatial resolution of 25 m across Europe. This offset was

84   used to evaluate the difference between micro- and macroclimate across space and seasons and

85   finally enabled us to calculate mean annual and monthly temperatures for European forest

86   understories. We found that sub-canopy air temperatures differ substantially from free-air

87   temperatures, being on average 2.1°C (standard deviation ± 1.6°C) lower in summer and 2.0°C higher

88   (± 0.7°C) in winter across Europe. Additionally, our high-resolution maps expose considerable

89   microclimatic variation within landscapes, not captured by the gridded macroclimatic products. The

90   provided forest sub-canopy temperature maps will enable future research to more accurately model

91   below-canopy biological processes and patterns, as well as species distributions.

92   **Keywords:** biodiversity, boosted regression trees, climate change, ecosystem processes, forest

93   microclimate, SoilTemp, species distributions, thermal buffering

3

94 **INTRODUCTION**

95 Climate change is having profound impacts on Earth's biodiversity and ecosystem processes (Lenoir et
96 al., 2020; Pecl et al., 2017; Scheffers et al., 2016). Ecological research assessing the consequences of
97 climate change is, however, largely based on coarse-gridded climate data of approximately 1 km² or
98 more (Lenoir et al., 2013; Willis & Bhagwat, 2009), such as WorldClim (1 km²; Fick & Hijmans, 2017),
99 CHELSA (1 km²; Karger et al., 2017), and TerraClimate (16 km²; Abatzoglou, Dobrowski, Parks, &
100 Hegewisch, 2018). For the terrestrial parts of the globe, these climatic grids are derived from
101 standardised meteorological stations recording weather conditions at approximately 2 meters height
102 in open and windy habitats to remove microclimatic effects (Jarraud, 2008). Consequently, these grids
103 are representative for long-term free-air temperatures (the "macroclimate") in open ecosystems.
104 However, many organisms experience temperatures that substantially deviate from those captured
105 by macroclimatic grids (Bramer et al., 2018; De Frenne et al., 2019). These so-called microclimatic
106 temperatures play a crucial role in dictating biological and ecological processes close to the ground
107 surface such as vegetation, carbon and nutrient dynamics and species distributions (Lembrechts, Nijs,
108 & Lenoir, 2018; Nilsson & Wardle, 2005; Perry, 1994).

109 The available coarse-grained macroclimate data have been shown to fall short in its ability to
110 capture small-scale biological and physical processes close to the ground surface (Lembrechts et al.,
111 2019; Lenoir, Hattab, & Pierre, 2017). For example, most plants are responding to microclimatic
112 temperatures near the ground surface rather than free-air temperatures at 2 m height, and it has been
113 shown that the currently available macroclimate data inaccurately reflect the distribution of these
114 species (Lembrechts et al., 2019). This may lead to erroneous predictions of species range dynamics
115 (Lembrechts et al., 2018). The core of this problem is twofold. Firstly, macroclimatic grids do not
116 consider many climate-forcing factors operating near the ground surface. The ground and canopy
117 surfaces absorb solar radiation, and low wind speeds reduce thermal mixing of the air, leading to
118 significant fine-scale vertical and horizontal variation in air temperature (Geiger, 1950; Monin &
119 Obukhov, 1954; Richardson, 1922). Secondly, data readily available from global macroclimatic grids
120 consider the Earth to be a homogeneous surface of short vegetation with shading consistent with that
121 of a weather station. However, microclimates are arguably nowhere more evident than in forests,
122 where the amount of sunlight reaching the ground surfaces and absorbed by leaves varies
123 substantially owing to the structural complexity of forest canopies and significant variation in
124 evapotranspirative cooling (Bramer et al., 2018; De Frenne et al., 2019; Lenoir et al., 2017).
125 Furthermore, landscapes characterized by considerable topographic variation (e.g. slope, aspect,
126 elevation) have shown to harbour ample microclimatic variation (Lenoir et al., 2013; Macek, Kopecký,

4

127   & Wild, 2019) due to the effect of topography on processes such as cold-air drainage, incident solar

128   radiation and hydrology (e.g. soil moisture).

129   Although not a new discipline, microclimate ecology has gained renewed interest over the

130   past years (Bramer et al., 2018; De Frenne et al., 2021), providing the scientific community with many

131   insights on the processes underlying microclimate variability, especially related to the implications of

132   climate change. For example, several mechanistic models are available to derive microclimatic

133   temperatures (Kearney & Porter, 2017; Kearney et al., 2014; Maclean, 2019). Other studies make use

134   of an empirical design, in which a network of microclimate temperature loggers is installed within a

135   certain region to cover large environmental gradients (Frey et al., 2016; George, Thompson, &

136   Faaborg, 2015; Govaert et al., 2020; Greiser, Meineri, Luoto, Ehrlén, & Hylander, 2018; Macek et al.,

137   2019; Meeussen et al., 2021). Nonetheless, when moving to the continental extent, these methods

138   often reach their limitations. Although mechanistic models are capable of making accurate predictions

139   at high spatiotemporal resolutions across restricted spatial extents, they struggle to do this over large

140   spatial extents at high spatial resolution, as the processes must be modelled in hourly time-steps and

141   are thus more computationally intensive than their statistical counterparts (Maclean, Mosedale, &

142   Bennie, 2019). Moreover, the unpredictable nature of wind gusts underneath heterogeneous forest

143   canopies, and the effects of these on temperature gradients, makes it challenging to develop

144   mechanistic models of below-canopy microclimates (Landuyt et al., 2018). On the other hand,

145   empirical data from regional logger networks had not yet been combined within one database until

146   very recently (Lembrechts et al., 2020). To better model ecosystem functioning and predict the effects

147   of climate change on organisms living close to the Earth's surface, gridded microclimate data with a

148   broad geographical extent are thus urgently needed (Körner & Hiltbrunner, 2018; Lembrechts &

149   Lenoir, 2020; Zellweger et al., 2019). Yet, the spatiotemporal resolution used to define microclimate

150   is organism specific (Potter, Woods, & Pincebourde, 2013) and fractal by nature. This means that the

151   fractal dimension, in terms of spatiotemporal resolution, of microclimate as experienced by

152   understory plants, for instance, might be orders of magnitude larger than the fractal dimension of

153   microclimate as experienced by smaller organisms, like insects living in tree holes or dead wood

154   (Pincebourde & Woods, 2020).

155   To help fill this critical knowledge gap, the SoilTemp global database of soil and near-surface

156   temperature time series has recently been launched (Lembrechts et al., 2020), collecting *in situ*

157   temperature logger data from regional microclimate logger networks in various habitats across the

158   globe. The currently available time series from 1,248 aboveground temperature sensors across

159   European forests provide a unique opportunity to accurately predict sub-canopy forest temperature

160   at a continental scale and at a spatial resolution that matters for organisms living in the forest

161 understory. Here, given our focus on the forest floor, we decided to work with a spatial resolution of

162 25 m. Not only for practical reasons (i.e. resolution at which predictor variables are available at a

163 continental extent), but also for ecological reasons as this is the scale at which both foresters (i.e.

164 forest inventories usually use plots ranging between 625 and 1,000 m²) and botanists (i.e. forest

165 vegetation surveys usually use 100 to 500 m² plots) work to describe the forest understory in the field.

166 For this, we calculated the mean monthly temperature offset between microclimate temperature,

167 based on *in situ* temperature measurements from the SoilTemp database (Lembrechts et al., 2020),

168 and macroclimate temperature, based on ERA5-Land reanalysis data (Muñoz-Sabater et al., 2021).

169 This offset was then related to different variables (i.e. topographical, biological and macroclimatic) to

170 quantify the difference between micro- and macroclimate across space and seasons and to derive

171 gridded microclimate products that are meaningful for studying biodiversity on the forest floor.

172 Moreover, the offset enables us to (i) model average sub-canopy temperatures over a 20-year period

173 and (ii) quantify the buffering capacities of forests across Europe, where buffering is defined as a

174 dampening of the macroclimate, such that temporal fluctuations related to the macroclimate still

175 exist, yet much less pronounced than outside of the forest (De Frenne et al., 2021).

176   **METHODS**

177   **Data acquisition**

178   *In situ* microclimatic temperature measurements were compiled in SoilTemp, a global database of soil

179   and near-surface air temperature measurements combining both published and unpublished data

180   sources (Lembrechts et al., 2020). Firstly, we only included measurement locations within European

181   mainland forest habitats, defined as all tree elements detectable from multispectral high resolution

182   (20 m) satellite (Sentinel-2, Landsat 8) imagery (European Union, 2020) in all 27 EU countries, plus

183   Albania, Bosnia and Herzegovina, Kosovo, Liechtenstein, Montenegro, North Macedonia, Norway,

184   Serbia, the United Kingdom and Switzerland. Secondly, we selected near-surface air temperature

185   measurements at a height between 0-100 cm above ground from time series spanning at least one

186   month with a temporal resolution of less than four hours. Measurements taken at the same location,

187   but at different heights, were included as separate data points while keeping track of logger ID to

188   account for potential pseudo-replication issues (i.e. when dividing data in training and testing bins for

189   cross-validation). This resulted in 1,248 time series at 1,092 locations, extending over the period from

190   2000 to 2020 and geographically spanning a latitudinal gradient over Europe from Portugal (38.54N

191   8.00W) to Sweden (64.11N 19.45E) and a longitudinal gradient from Portugal (38.64N 8.60W) to

192   Finland (62.33N 30.37E; Supplementary Figure 1a). Note that different sensor and shielding

193   combinations were used within the input data and that they might contribute to errors in the model

194   (Supplementary Table 1). However, experimental research has shown that such errors are relatively

195   small in shaded environments such as forests (Maclean et al., 2021), an order of magnitude smaller

196   than the measured offsets.

197   Next, we aggregated the time series, usually available at hourly or sub-daily (e.g. every two or

198   four hours) native resolutions, to mean monthly temperatures, after visually checking each time series

199   for outliers and erroneous data. We further only selected months with at least 28 days of data,

200   resulting in a cumulative 24,291 months of near-surface air temperature (Supplementary table 2).

201   **Offset calculation**

202   We derived a monthly temperature offset value (ΔT = sub-canopy T°C − free-air T°C) between

203   microclimate (i.e. sub-canopy) and macroclimate (i.e. free-air) temperature measurements in order

204   to relate this ΔT to different explanatory variables and quantify the difference between micro- and

205   macroclimate across space and seasons. Positive offset values thus indicate, on average, warmer

206   forest microclimate conditions, whereas negative values point to a colder forest microclimate. The

207   offset (ΔT) was calculated as the difference between the monthly mean microclimate temperature, as

208   measured by the loggers, and the corresponding monthly mean air temperature value at 2 m height

7

209   for exactly the same month, year and grid cell from ERA5-Land reanalysis data with a spatial resolution

210   of 0.1 × 0.1 degrees (Muñoz-Sabater et al., 2021).

211   **Acquisition of covariate layers**

212   Covariates were selected based on their known relevance for forest microclimatic temperatures

213   according to literature (Greiser et al., 2018; Zellweger et al., 2019), spatial resolution and availability

214   at the continental scale. In total, twenty covariate layers were selected to create a covariate layer

215   stack, including topographical, biological and macroclimatic variables.

216   Topographic layers were derived from a digital elevation model (EU-DEM v1.1) at 25 m

217   resolution (European Union, 2020). Both northness and eastness were derived as the cosine and sine

218   of the aspect (°), respectively. Additionally, we incorporated slope (°), elevation (m a.s.l.) and latitude

219   to account for the variation in incoming solar radiation (Lenoir & Svenning, 2013; Meineri & Hylander,

220   2017). Relative elevation (m) represents the elevational difference between each pixel and the lowest

221   pixel within a 500 m buffer. This is often used as a proxy for cold air drainage, as cold air moves

222   downslope (Ashcroft & Gollan, 2013). Distance to the coast was included because the heat capacity of

223   the ocean has an important effect on (microclimatic) temperatures (Vercauteren, Destouni, Dahlberg,

224   & Hylander, 2013; Zellweger et al., 2019). Furthermore, the effect of increased water vapour content

225   in the atmosphere near the coast affects cloud patterns which, in turn, influence incoming solar

226   radiation (Zellweger et al., 2019). Finally, the topographic wetness index (TWI) was used as a proxy for

227   soil moisture (Meineri, Dahlberg, & Hylander, 2015). The index quantifies the effect of topographic

228   variation on hydrological processes by taking into account both slope and specific catchment area

229   (Beven & Kirkby, 1979). We calculated TWI by using the *Freeman FD8* flow algorithm with a flow

230   dispersion of 1.0, a flow width equal to the raster cell size (i.e. 25 m) and a local slope gradient

231   (Kopecký, Macek, & Wild, 2021).

232   The 2015 high resolution (20 m) Copernicus maps of tree cover density (%), which refers to

233   the percentage of tree cover per raster cell, and forest type (broadleaf *vs*. coniferous) were included.

234   To quantitatively capture the phenological differences between broadleaved and coniferous forests,

235   we calculated two NDVI values, representative for winter (December-February) and summer months

236   (June-August). NDVI variables were derived from Landsat 4, 5, 7 and 8 satellite images over a period

237   from 2000-2020 provided in Google Earth Engine (Gorelick et al., 2017). Each image underwent pre-

238   processing by converting low-quality data (e.g. due to presence of clouds, snow or shadows) into

239   missing values based on the masks provided with the downloaded images.

240   Furthermore, long-term average macroclimatic conditions were considered by including four

241   WorldClim bioclimatic variables covering the period between 1970 and 2000 (Fick & Hijmans, 2017):

242   BIO1 (Mean Annual Temperature), BIO5 (Maximum Temperature of the Warmest Month), BIO6

243   (Minimum Temperature of the Coldest Month) and BIO12 (Annual Precipitation). These were chosen

244   due to the specific interaction of these variables with some of the topographical and biological

245   variables. For instance, Greiser et al. (2018) found that forest density was an important driver for

246   minimum and maximum microclimate temperatures in summer, whereas topography had a stronger

247   influence on extreme temperatures in autumn and winter. Furthermore, mean annual cloud cover (%)

248   over 2000-2014 derived from MODIS products was included to account for the effect of cloud cover

249   on incoming solar radiation (Wilson & Jetz, 2016). Annual snow cover probability (%) was derived as

250   the average of monthly snow probability based on a pixel-wise frequency of snow occurrence (snow

251   cover > 10%) in MODIS daily snow cover products (MOD10A1 & MYD10A1; Hall, Riggs, Salomonson,

252   DiGirolamo, & Bayr, 2002) over 2001-2019. Finally, we also included the sensor height above the

253   ground surface as a covariate in our models as this significantly impacts the magnitude of the

254   temperature offset (De Frenne et al., 2019; Geiger, 1950).

255   When necessary, covariate map layers were reprojected and resampled to an equal area

256   projection in EPSG:3035 (ETRS89-extended / LAEA Europe) at 25 m resolution using bilinear

257   interpolation for quantitative data and the nearest neighbour method for categorical data. We present

258   variable importance quantitatively and the relationship between each covariate and the response

259   visually in partial dependence plots (Supplementary Figure 2). Furthermore, we show the strongest

260   two- and three-way interactions among covariates (Supplementary Figure 3).

261   **Geospatial modelling**

262   Machine-learning techniques often outperform other statistical techniques such as generalized linear

263   models (GLMs) or generalized additive models (GAMs) in terms of predictive power (Appelhans,

264   Mwangomo, Hardy, Hemp, & Nauss, 2015). As we aim to maximize predictive power within the

265   environmental space covered by our data rather than explanatory power, we used boosted regression

266   trees (BRTs), also referred to as gradient boosting machine, to model the relationship between the

267   selected covariates and ΔT (Appelhans et al., 2015; Elith, Leathwick, & Hastie, 2008). Especially for

268   regression, BRTs are particularly valuable due to their capacity to uncover nonlinear relationships as

269   well as their automatic detection of complex interactions among covariates (Supplementary Figure 3).

270   Furthermore, this algorithm is capable to handle multicollinearity among covariates (Supplementary

271   Figure 4), outliers and missing data. On the other hand, BRTs are prone to (i) overfitting due to

272   sequential fitting of trees (Elith et al., 2008) and (ii) errors when extrapolating outside the boundaries

273   of the training data. To deal with these issues, we (i) implemented model regularization by means of

274   low learning rate values (0.1-0.001) and cross-validation (Elith et al., 2008) while also (ii) providing a

275   map indicating where the model is extrapolating beyond the values of the training data.

9

276   BRTs were built using the *gbm* R package (Ridgeway, 2005). We searched for the optimal

277   hyperparameter values with the *caret* package (Kuhn, 2012) by means of a grid search over the

278   possible values of the four hyperparameters: interaction depth (2-6); total number of trees (100-

279   10,000); learning rate (0.1-0.001); and the minimal observations in each terminal node (8-12) (Elith et

280   al., 2008). In total, 14,925 models were evaluated by 10-fold cross-validation (CV) while (i) taking into

281   account logger ID to avoid pseudo-replication between folds and (ii) stratifying by the biogeographical

282   regions of Europe (Cervellini et al., 2020), meaning that each fold contained 10% of the loggers in each

283   biogeographical region. Finally, optimal hyperparameter values were selected by maximizing R^2_{CV}.

284   Once the optimal hyperparameters were determined, we applied a stratified bootstrap

285   approach to fit 30 different models (van den Hoogen et al., 2019). The bootstrapping procedure each

286   time randomly sampled the data with replacement to fit the model. The biogeographical regions of

287   Europe (Cervellini et al., 2020) were used as stratum for the random sampling to ensure that every

288   biogeographical region was proportionally represented according to data availability in each region.

289   Each of the bootstrapped models made separate predictions for each month – that is 3,141,115,825

290   European forest pixels classified 360 times (12 months × 30 bootstraps). Model precision was then

291   quantified by calculating, per pixel, a 95% confidence interval (mean ± 1.96 SE) for each month. We

292   predicted temperature at 15 cm height as this is the most common height within the input data

293   (Supplementary Table 2). Furthermore, most understory forest plant species (e.g. herbs, grasses,

294   sedges and ferns) fit, on average, to this height.

295   Machine-learning techniques, like BRTs, are known to be less capable to extrapolate beyond

296   the boundaries set by the environmental variables in the original training data. To assess where our

297   model is extrapolating – and thus possibly providing less reliable predictions – we calculated for each

298   pixel the percentage of quantitative covariate layers for which the pixel value lies outside the range of

299   data covered by the dataset. Finally, we used a spatial leave-one-out cross-validation analysis to test

300   the effect of spatial autocorrelation in the dataset (Supplementary Figure 5; Roberts et al., 2017; van

301   den Hoogen et al., 2021). This approach each time validates a model on data from one distinct location

302   and trains a model on the remaining data. This is repeatedly done for each of our 1,092 locations.

303   Because of potential spatial autocorrelation close to the validation location, this process is repeated

304   with an increasing buffer around the validation location, each time excluding data points that fall

305   within the defined buffer zone from the training data. This method allows assessing if the R^2 stabilizes,

306   an indication of limited spatial autocorrelation.

307   **Offset and forest microclimate temperature maps at 25 m resolution**

308   Here, we make the European monthly temperature offset grids available as open data. These can, in

309   turn, be used to convert gridded macroclimate products into gridded microclimate products. We

10

310   opted to illustrate the calculation of the mean annual forest microclimatic temperature (further

311   referred to as "forestBIO1") but this calculation can be carried out for all other temperature-related

312   bioclimatic variables from BIO1 to BIO11 (Fick & Hijmans, 2017; Karger et al., 2017). Firstly, we

313   calculated (i) the mean annual temperature offset as the average of the monthly offset maps and (ii)

314   the mean annual temperature over 2000-2019 from monthly TerraClimate data (Abatzoglou et al.,

315   2018). Secondly, we calculated forestBIO1 by adding anomalies of the predicted mean annual offset

316   to the corresponding TerraClimate mean annual temperature map (Abatzoglou et al., 2018).

317   All calculations were performed in R version 4.0.2 (R Core Team, 2020). The *Tier-2 Genius*

318   cluster from the high-performance computing facilities of Flanders was used to perform the

319   calculations.

320   **RESULTS AND DISCUSSION**

321   **ForestTemp – microclimatic temperature maps of European forests**

322   Our bootstrapped models for monthly temperature offset performed well with a coefficient of

323   determination (R^2) of 0.79 (95% CI: 0.78-0.80), a root mean square error of 1.19°C (1.17°C – 1.21°C)

324   and a mean absolute error of 0.87°C (0.85°C – 0.89°C). The spatial leave-one-out cross-validation also

325   showed reasonably good predictive performance with R^2 stabilizing around 0.55 when increasing the

326   buffer size above 100 km (Supplementary Figure 5). Mean monthly temperature offsets at 15 cm

327   above ground over 30 bootstrap iterations ranged between -2.5°C and 10.8°C in January and from -

328   5.8°C to 3.2°C in July (Supplementary Table 3). Model predictions described expected patterns in ΔT,

329   with forest microclimates overall being warmer than the macroclimate during winter, and colder

330   during summer (Figure 1). This corresponds to earlier findings for temperate systems, where forests

331   act as a thermal insulator: on average cooling the understory by 2.1°C in summer and warming it by

332   2.0°C in winter compared to monthly free-air temperature (De Frenne et al., 2019; Geiger, 1950). Our

333   model was also able to capture the phenological difference between broadleaved and coniferous

334   forests. We found bimodal peaks in winter, particularly pronounced in January (Figure 2), with

335   temperature offsets in coniferous forests, on average, 1.0°C warmer (Supplementary Figure 6). This

336   likely relates to the differences in tree cover density between these two forest types during that time

337   of year. The observed pattern can further be caused by the fact that coniferous forests are, at the

338   continental scale, more abundant in places with snow, which is known to act as an additional thermal

339   insulator (Aalto, Scherrer, Lenoir, Guisan, & Luoto, 2018). Mean annual temperature offset ranged

340   between -5.7°C and 7.8°C, which translates into a mean annual forest microclimate temperature

341   (forestBIO1) between -2.0°C and 22.1°C across Europe (Figure 3), compared to mean annual

342   macroclimate temperature ranging between -3.5°C and 20.4°C.

343   The bootstrapped models turned out robust, as standard errors were generally small

344   compared to the modelled temperature offsets: standard errors of the mean of monthly temperature

345   offsets stayed below 0.6°C in most months and across most parts of Europe (Figure 4, Supplementary

346   Table 3). Higher standard errors are noticed when predicting the offset at very high (above mid-

347   Sweden) and very low latitudes (southern Spain) as well as in high-elevational regions, which are

348   expected to be caused by extrapolation outside the environmental gradient covered by the availability

349   of temperature loggers installed in forest ecosystems (Figure 5a; Supplementary Figure 1b). The

350   overall precision of each prediction is represented by the width of the 95% confidence interval for

351   each pixel (Figure 5b), which reaches 2.5°C in winter (January) and 1.2°C in summer (July,

352   Supplementary Table 3).

353   As for any other machine learning technique, we caution against the use of data from regions

354   where the model is extrapolating (mainly in southern Spain, high elevations areas of the Alps and

355   Scandinavia, Figure 5a). As with any spatial model, our model is calibrated on certain environmental

356   conditions, and predictions outside these conditions might induce errors. This problem partly stems

357   from undersampled regions in the database (e.g. southern Spain, the United Kingdom, large parts of

358   eastern Europe and high-elevation forested areas) which should be a scope of future research. The

359   extrapolation (Figure 5a) and precision (Figure 5b) maps could therefore be used as spatial masks to

360   remove or downweight the pixels for which predictions are beyond the range of values covered by the

361   models or unprecise.

362   **Drivers of microclimate**

363   As expected, seasonality (i.e. month of the year) plays a crucial role in defining the direction of the

364   monthly temperature offset, overall being positive in autumn and winter and negative during spring

365   and summer (Supplementary Figure 2). Bioclimatic variables seem to be important covariates, with

366   the exception of mean annual temperature due to its high collinearity with other climatic variables

367   (Supplementary Figure 4). However, we notice an overall negative relationship between the offset and

368   mean annual temperature (Supplementary Figure 2), which might be related to the predicted

369   decoupling of forest microclimate warming from warming of the free air (De Frenne et al., 2019; Lenoir

370   et al., 2017). However, global warming-related disturbances like extreme droughts, pest outbreaks

371   (e.g. pathogens, bark beetles) and increased fire incidence could nullify the insulation capacity of the

372   forest canopy, disrupting this low coupling. Furthermore, the high importance of distance to the coast

373   and mean annual precipitation suggest an important role for water (McLaughlin et al., 2017). On the

374   one hand, temperature buffering is a function of local soil moisture, which in turn can be driven by

375   distance to water bodies and precipitation (Davis, Dobrowski, Holden, Higuera, & Abatzoglou, 2019).

376   For instance, it is the effect of increased water vapour content in the atmosphere near the coast which

377   affects cloudiness, which in turn is an important variable as it affects shading and incoming solar

378   radiation. On the other hand, moisture can have an impact on different levels by increasing the

379   vegetation or snow cover. Besides, snow also seems to be important in driving the temperature offset

380   (Aalto et al., 2018). The interaction between snow cover and sensor height (Supplementary Figure 3c)

381   clearly hints towards an insulating effect of snow on the sensor which is, contrary to standardised

382   meteorological stations, not kept free of snow or ice. We thus expect that large positive wintertime

383   offsets in regions with high snow cover probability (i.e. high-latitudinal and high-elevational regions)

384   are mainly caused by this snow insulating effect. Of moderate importance are topographic variables

385   such as slope and elevation which show a positive and negative relationship with ΔT, respectively.

386   Moreover, sensor height, with a clear positive effect on ΔT, and the NDVI play an intermediate role.

387   Surprisingly, biotic variables such as tree cover density or forest type seem to be less good predictors

388   for the offset at the continental scale. However, the spatial resolution of 25 m used here is probably

389   still too coarse to capture these effects (Kašpar et al., 2021). More importantly, the availability of

390   accurate stand-level data at 25 m resolution (e.g. basal area, stem density, leaf area density or tree

391   height) is still limited. Airborne or terrestrial LiDAR-derived variables could be a valuable source of

392   data to solve these issues in the future (Frey et al., 2016; George et al., 2015; Kašpar et al., 2021).

393   However, just like with mean annual temperature, these effects might be partially captured by or

394   confounded with the combination of seasonality and NDVI.

395   Note that we do not intend to unravel the physical mechanisms driving the offset between

396   forest microclimate temperatures and free-air temperature. We are aware that most of our

397   explanatory variables (e.g. tree cover density, northness or slope) rather affect physical mechanisms

398   driving the offset (e.g. incoming solar radiation, wind speed) than sub-canopy temperatures directly

399   (Bennie, Huntley, Wiltshire, Hill, & Baxter, 2008). However, as we aim to create continental high-

400   resolution sub-canopy temperature maps for understory vegetation in European forests, a few strong

401   correlative relationships could be better than complex, physical models that are computationally

402   difficult to run at the continental extent and at high spatiotemporal resolution. Additionally, some

403   potentially important variables are not incorporated within our models, either due to the limited

404   availability or coarse spatial resolution of those variables. One of the possible limitations of our study

405   is the assumption that forests, and their characteristics, are static over time. However, large parts of

406   European forests are managed (Senf & Seidl, 2021), which makes it virtually impossible to incorporate

407   up-to-date vegetation variables such as forest height, basal area or age. Furthermore, although we

408   incorporated snow cover probability in the model, which shows an important interaction with sensor

409   height, we do need the exact snow height and duration at high spatiotemporal resolution to quantify

410   the insulation effect of snow on the logger sensors at different heights (Gisnås, Westermann, Schuler,

411   Melvold, & Etzelmüller, 2016). Unfortunately, data on snow water equivalent, needed to calculate

412   snow height and duration, are only available at a coarse spatial resolution of 5 km². Incorporating this

413   into the model would not substantially capture the effect as there is still high, fine-scale spatial

414   variability within each pixel. In addition, given the strong correlation of fine-scale snow dynamics with

415   topography, inclusion of the latter is likely to partially capture this effect (Aalto et al., 2018; Niittynen

416   & Luoto, 2018).

417   Finally, the 25 m spatial resolution is a significant step forward compared to existing

418   microclimate products across large spatial extents. Nonetheless, we have to acknowledge the

419   remaining within-pixel variability, due to the fractal nature of microclimates, both in spatial and

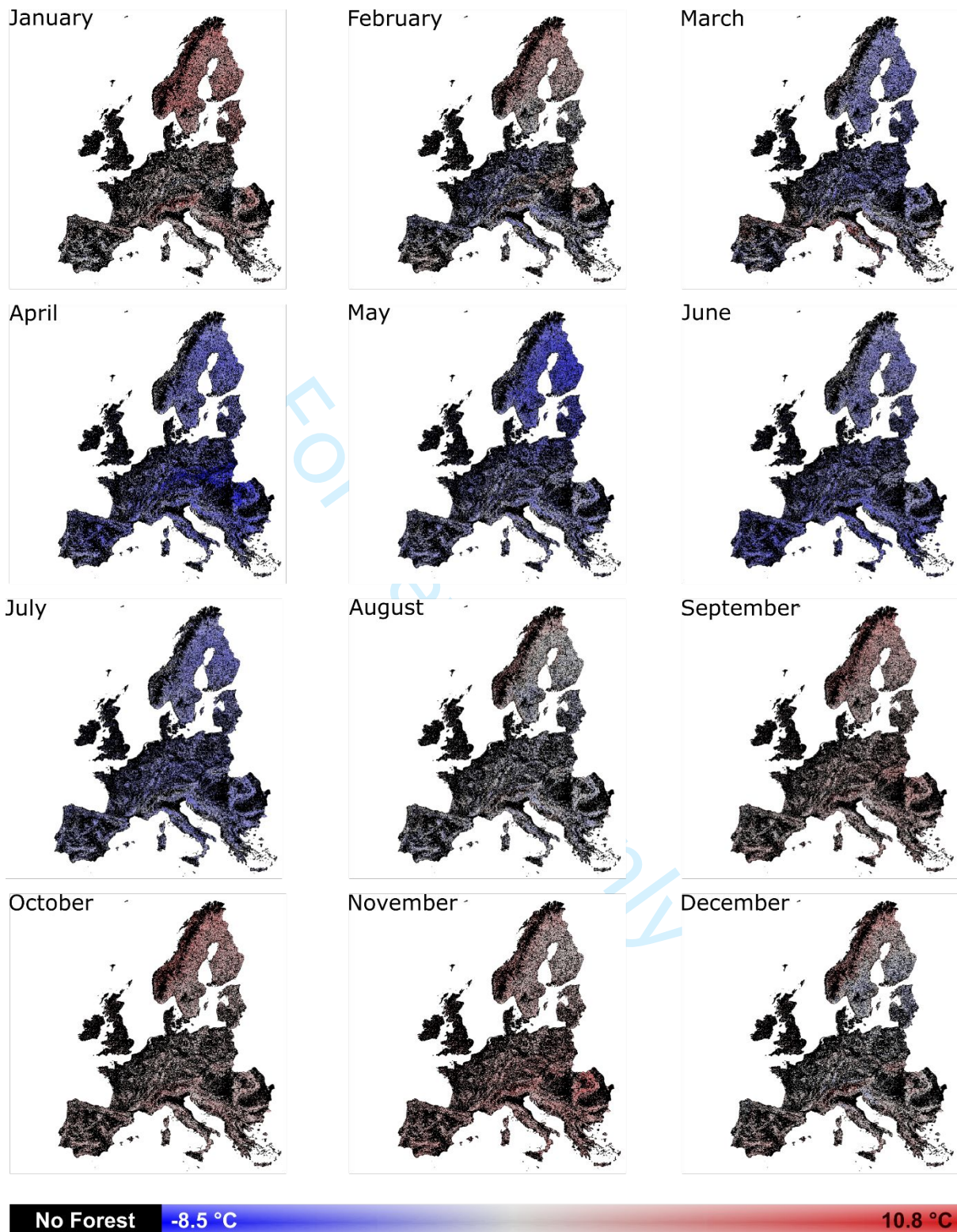420   temporal terms. Moreover, we know that some organisms, depending on their body size, utilize

421   microclimatic variation at orders of magnitude less than the spatiotemporal resolution used in this
422   study. For instance, small insects can use sunflecks and microhabitats (tree holes and dead wood)
423   available within a 25 m × 25 m grid cell to seek micro-variation in temperature throughout the course
424   of the day. Hence, recent research argues in favour of incorporating especially higher temporal
425   resolutions in ecological analyses (Bütikofer et al., 2020). However, given current-day data availability
426   and computational power as well as our focus on the forest floor, this study mapped microclimates at
427   a continental scale according to the state-of-the-art.

428   **Applications and future perspectives**

429   The outcomes of this study allow researchers to use accurate forest microclimate temperature data
430   in large-scale analyses. This is an important step forward as the mismatch between macro- and
431   microclimate forest temperatures is substantial and can thus seriously bias the outcome of ecological
432   and global change studies. For example, microclimate-informed species distribution models (SDM;
433   Lenoir et al., 2017) could reveal more accurate insights into the various processes underlying species
434   vulnerability to climate change on different aspects, including climate change exposure, sensitivity,
435   adaptability and dispersal (Pacifici et al., 2015). Climate change exposure can be buffered by
436   microclimate whereas climate sensitivity impacts a species' ability to cope with microclimatic
437   warming. Furthermore, microclimatic variation affects the spatial distribution of adaptive genetic
438   variation and thus the ability of a population to survive climate change (De Kort et al., 2020; Graae et
439   al., 2018). Finally, microclimate drives the spatial distribution of dispersal pathways throughout the
440   landscape and thus directly impacts dispersal ability and populations in fragmented landscapes.
441   Understanding how these processes interact with microclimate to shape species responses and their
442   vulnerability to climate change is fundamental to predicting range dynamics.

443   We trust the predicted thermal offsets for forest ecosystems and their possibility to derive
444   gridded microclimate products will enable future research to more correctly model ecological
445   processes and patterns in the forest understory, as well as forest-dwelling species distributions
446   affected by climate change. These maps are available as GeoTIFFs for download through figshare (doi:
447   10.6084/m9.figshare.14618235) and will be updated as more or better data become available.
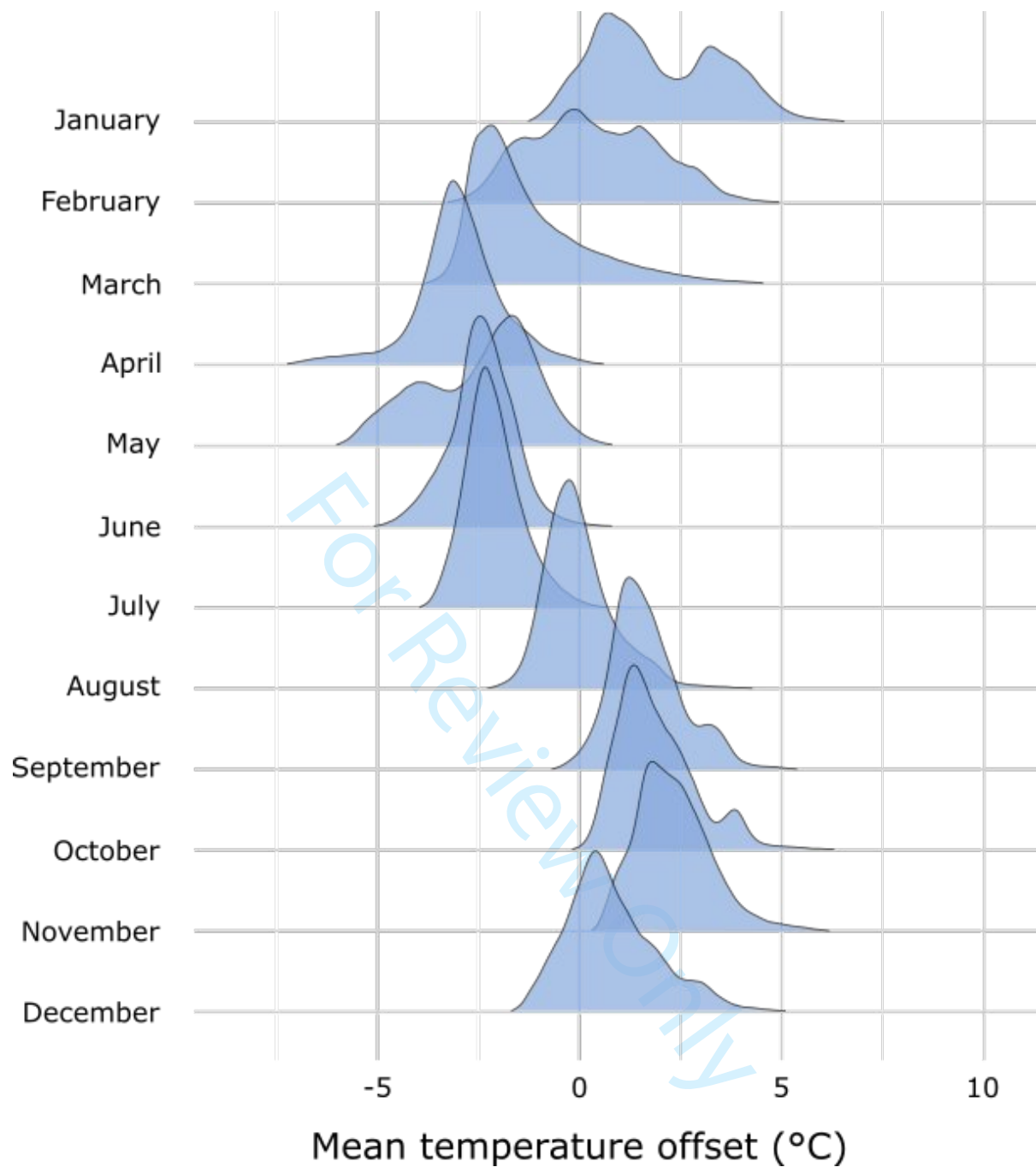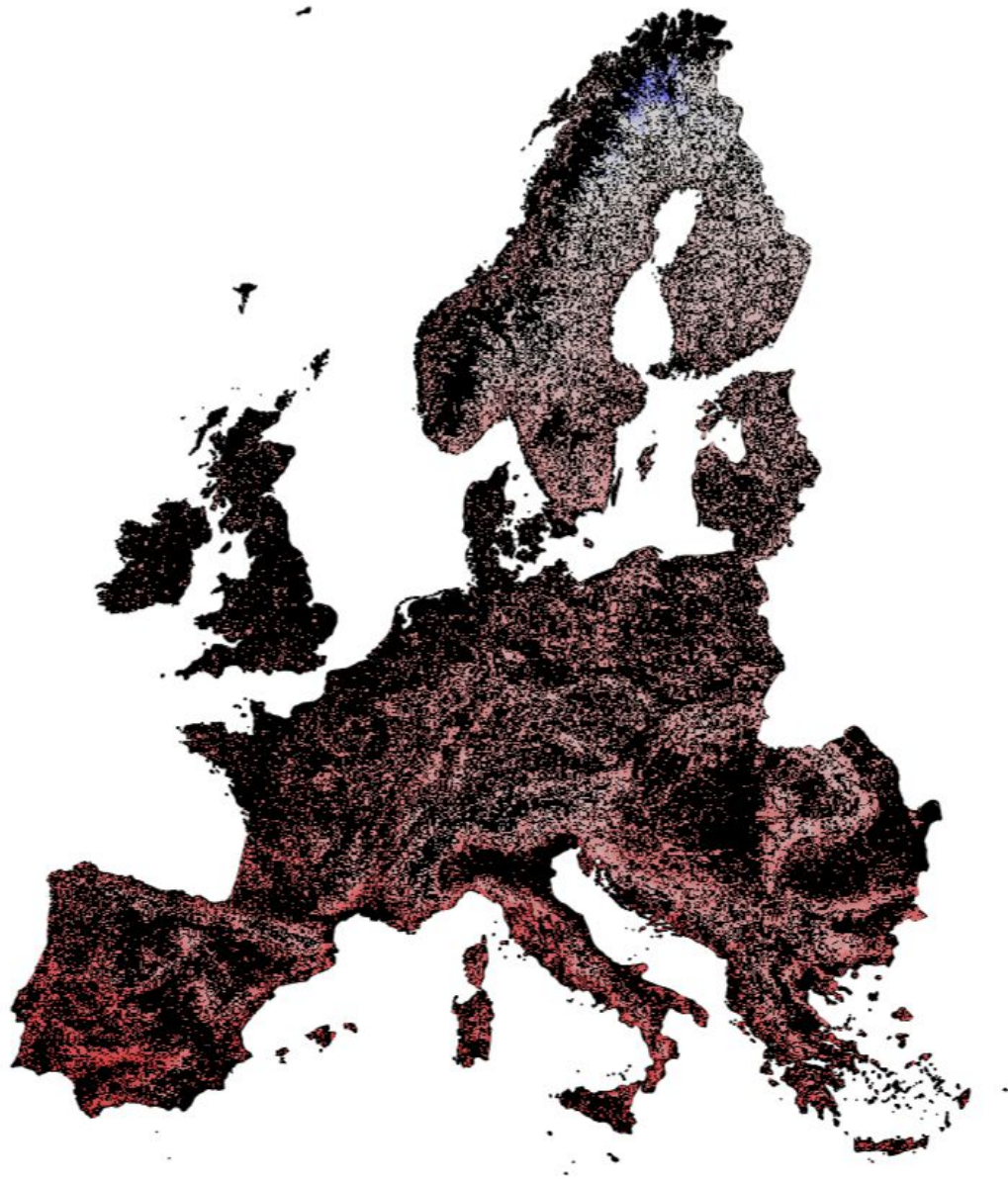
448 **FIGURES**

January February March
April May June
July August September
October November December

No Forest   -8.5 °C   10.8 °C

449

450 *Figure 1: Predicted mean monthly air temperature offset across European forests.* *Mean monthly temperature*
451 *offset at 15 cm above ground between in-situ forest microclimate and free-air temperatures (sub-canopy T°C*
452 *minus free-air T°C) (in °C).*

453

Figure 2: Histograms of mean monthly temperature offsets. *Density ridgeplots for the monthly temperature*
offset at 15 cm above ground between in-situ forest microclimate and free-air temperatures (sub-canopy T°C –
free-air T°C) (in °C) indicating, per month, the distribution of 1,000,000 randomly sampled raster pixel values
across European forests.

459 **Figure 3: forestBIO1.** *Mean annual temperature at 15 cm above ground in European forests (in °C) with a spatial*
460 *resolution of 25 m, representative of the 2000-2020 period, calculated using the maps of monthly mean air*
461 *temperature offsets at 25 m resolution (Figure 2) added to the mean annual air temperature from TerraClimate*
462 *at 4 km resolution.*

463
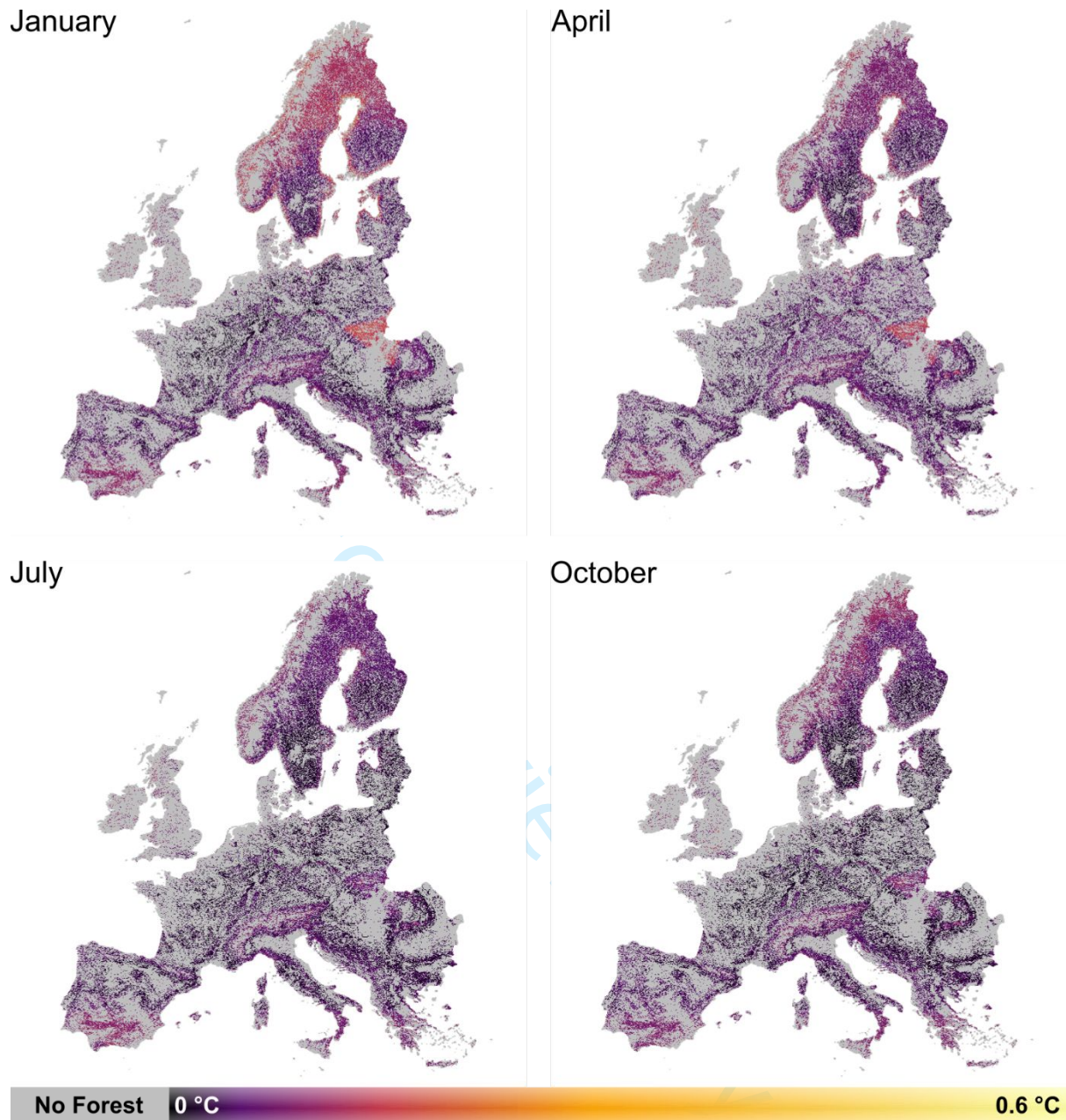
Figure 4: Robustness of the temperature offset model at 15 cm above ground across European forests. *Standard errors of the mean from predicted mean monthly temperature offsets (sub-canopy T°C minus free-air T°C) at 15 cm above ground derived from 30 bootstrapped models (in °C). For additional months, see supplementary Figure 7. See Supplementary Table 3 for detailed quantitative data.*

468
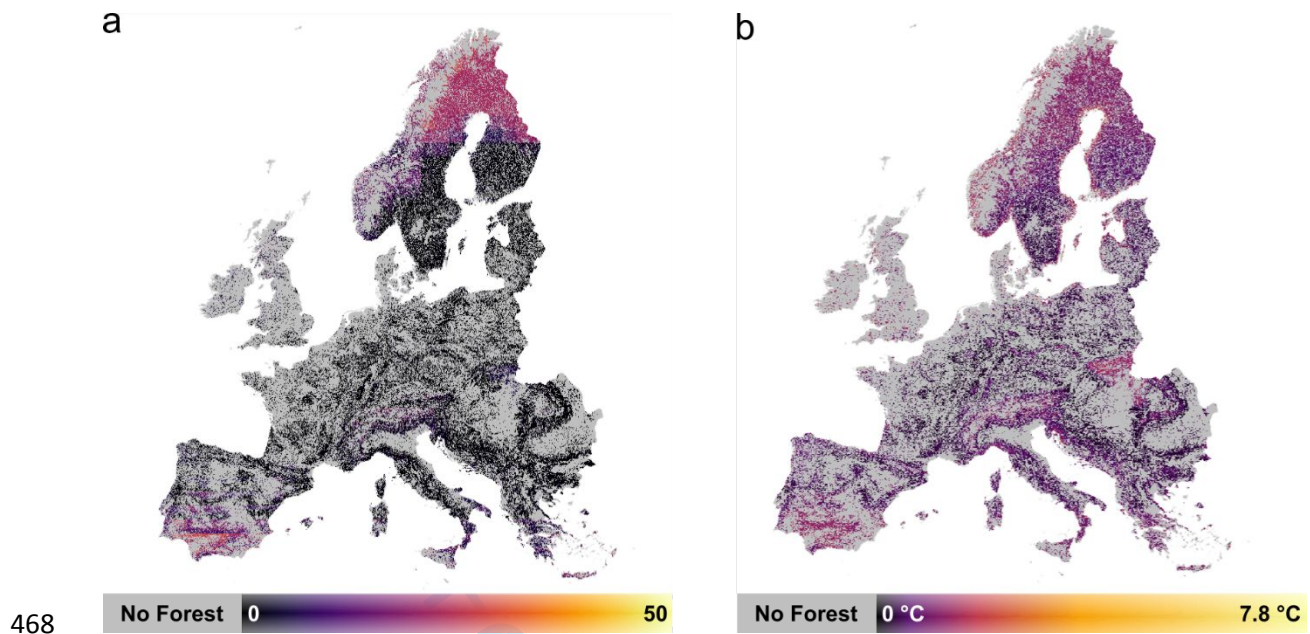
469 **Figure 5: Extrapolation and precision maps.** *(a) The percentage of quantitative variables for which the pixel lies*
470 *outside the range of data covered by the training data. Pixels with high values indicate that the model has to*
471 *extrapolate for many of the covariates for that specific pixel (i.e. due to missing in-situ measurements). (b)*
472 *Precision of predictions for each pixel, calculated as the width of the bootstrapped 95% confidence interval for*
473 *each pixel.*

REFERENCES

Aalto, J., Scherrer, D., Lenoir, J., Guisan, A., & Luoto, M. (2018). Biogeophysical controls on soil-atmosphere thermal differences: implications on warming Arctic ecosystems. *Environmental Research Letters*, *13*(7), 074003. https://doi.org/10.1088/1748-9326/aac83e

Abatzoglou, J. T., Dobrowski, S. Z., Parks, S. A., & Hegewisch, K. C. (2018). TerraClimate, a high-resolution global dataset of monthly climate and climatic water balance from 1958–2015. *Scientific Data*, *5*(1), 170191. https://doi.org/10.1038/sdata.2017.191

Appelhans, T., Mwangomo, E., Hardy, D. R., Hemp, A., & Nauss, T. (2015). Evaluating machine learning approaches for the interpolation of monthly air temperature at Mt. Kilimanjaro, Tanzania. *Spatial Statistics*, *14*, 91–113. https://doi.org/10.1016/j.spasta.2015.05.008

Ashcroft, M. B., & Gollan, J. R. (2013). The sensitivity of topoclimatic models to fine-scale microclimatic variability and the relevance for ecological studies. *Theoretical and Applied Climatology*, *114*(1–2), 281–289. https://doi.org/10.1007/s00704-013-0841-0

Bennie, J., Huntley, B., Wiltshire, A., Hill, M. O., & Baxter, R. (2008). Slope, aspect and climate: Spatially explicit and implicit models of topographic microclimate in chalk grassland. *Ecological Modelling*, *216*(1), 47–59. https://doi.org/10.1016/j.ecolmodel.2008.04.010

Beven, K. J., & Kirkby, M. J. (1979). A physically based, variable contributing area model of basin hydrology. *Hydrological Sciences Bulletin*, *24*(1), 43–69. https://doi.org/10.1080/02626667909491834

Bramer, I., Anderson, B. J., Bennie, J., Bladon, A. J., De Frenne, P., Hemming, D., … Gillingham, P. K. (2018). Advances in Monitoring and Modelling Climate at Ecologically Relevant Scales. *Advances in Ecological Research*, *58*, 101–161. https://doi.org/10.1016/BS.AECR.2017.12.005

Bütikofer, L., Anderson, K., Bebber, D. P., Bennie, J. J., Early, R. I., & Maclean, I. M. D. (2020). The problem of scale in predicting biological responses to climate. *Global Change Biology*, *26*(12), 6657–6666. https://doi.org/10.1111/gcb.15358

Cervellini, M., Zannini, P., Di Musciano, M., Fattorini, S., Jiménez-Alfaro, B., Rocchini, D., … Chiarucci, A. (2020). A grid-based map for the Biogeographical Regions of Europe. *Biodiversity Data Journal*, *8*. https://doi.org/10.3897/BDJ.8.e53720

Davis, K. T., Dobrowski, S. Z., Holden, Z. A., Higuera, P. E., & Abatzoglou, J. T. (2019). Microclimatic buffering in forests of the future: the role of local water balance. *Ecography*, *42*(1), 1–11. https://doi.org/10.1111/ecog.03836

De Frenne, P., Lenoir, J., Luoto, M., Scheffers, B. R., Zellweger, F., Aalto, J., … Hylander, K. (2021). Forest microclimates and climate change: Importance, drivers and future research agenda. *Global Change Biology*, (November 2020), gcb.15569. https://doi.org/10.1111/gcb.15569

531   De Frenne, P., Zellweger, F., Rodríguez-Sánchez, F., Scheffers, B. R., Hylander, K., Luoto, M., … Lenoir,

532   J. (2019). Global buffering of temperatures under forest canopies. *Nature Ecology & Evolution*,

533   *3*(5), 744–749. https://doi.org/10.1038/s41559-019-0842-1

534   De Kort, H., Panis, B., Helsen, K., Douzet, R., Janssens, S. B., & Honnay, O. (2020). Pre-adaptation to

535   climate change through topography-driven phenotypic plasticity. *Journal of Ecology*, *108*(4),

536   1465–1474. https://doi.org/10.1111/1365-2745.13365

537   Elith, J., Leathwick, J. R., & Hastie, T. (2008). A working guide to boosted regression trees. *Journal of*

538   *Animal Ecology*, *77*(4), 802–813. https://doi.org/10.1111/j.1365-2656.2008.01390.x

539   European Union. (2020). Copernicus Land Monitoring Service. *European Environment Agency (EEA)*.

540   Fick, S. E., & Hijmans, R. J. (2017). WorldClim 2: new 1-km spatial resolution climate surfaces for

541   global land areas. *International Journal of Climatology*, *37*(12), 4302–4315.

542   https://doi.org/10.1002/joc.5086

543   Frey, S. J. K., Hadley, A. S., Johnson, S. L., Schulze, M., Jones, J. A., & Betts, M. G. (2016). Spatial

544   models reveal the microclimatic buffering capacity of old-growth forests. *Science Advances*,

545   *2*(4), e1501392. https://doi.org/10.1126/sciadv.1501392

546   Geiger, R. (1950). *The climate near the ground*. Cambridge, Mass.: Harvard University Press. 482p.

547   pages.

548   George, A. D., Thompson, F. R., & Faaborg, J. (2015). Using LiDAR and remote microclimate loggers

549   to downscale near-surface air temperatures for site-level studies. *Remote Sensing Letters*,

550   *6*(12), 924–932. https://doi.org/10.1080/2150704X.2015.1088671

551   Gisnås, K., Westermann, S., Schuler, T. V., Melvold, K., & Etzelmüller, B. (2016). Small-scale variation

552   of snow in a regional permafrost model. *The Cryosphere*, *10*(3), 1201–1215.

553   https://doi.org/10.5194/tc-10-1201-2016

554   Gorelick, N., Hancher, M., Dixon, M., Ilyushchenko, S., Thau, D., & Moore, R. (2017). Google Earth

555   Engine: Planetary-scale geospatial analysis for everyone. *Remote Sensing of Environment*, *202*,

556   18–27. https://doi.org/10.1016/j.rse.2017.06.031

557   Govaert, S., Meeussen, C., Vanneste, T., Bollmann, K., Brunet, J., Cousins, S. A. O., … De Frenne, P.

558   (2020). Edge influence on understorey plant communities depends on forest management.

559   *Journal of Vegetation Science*, *31*(2), 281–292. https://doi.org/10.1111/jvs.12844

560   Graae, B. J., Vandvik, V., Armbruster, W. S., Eiserhardt, W. L., Svenning, J.-C., Hylander, K., … Lenoir,

561   J. (2018). Stay or go – how topographic complexity influences alpine plant population and

562   community responses to climate change. *Perspectives in Plant Ecology, Evolution and*

563   *Systematics*, *30*(September 2017), 41–50. https://doi.org/10.1016/j.ppees.2017.09.008

564   Greiser, C., Meineri, E., Luoto, M., Ehrlén, J., & Hylander, K. (2018). Monthly microclimate models in

565   a managed boreal forest landscape. *Agricultural and Forest Meteorology*, *250–251*(December

566   2017), 147–158. https://doi.org/10.1016/j.agrformet.2017.12.252

567 Hall, D. K., Riggs, G. A., Salomonson, V. V, DiGirolamo, N. E., & Bayr, K. J. (2002). MODIS snow-cover

568   products. *Remote Sensing of Environment*, *83*(1–2), 181–194. https://doi.org/10.1016/S0034-

569   4257(02)00095-0

570 Jarraud, M. (2008). *Guide to meteorological instruments and methods of observation (WMO-No. 8)*.

571   Geneva, Switzerland: World Meteorological Organisation.

572 Karger, D. N., Conrad, O., Böhner, J., Kawohl, T., Kreft, H., Soria-Auza, R. W., … Kessler, M. (2017).

573   Climatologies at high resolution for the earth's land surface areas. *Scientific Data*, *4*(1), 170122.

574   https://doi.org/10.1038/sdata.2017.122

575 Kašpar, V., Hederová, L., Macek, M., Müllerová, J., Prošek, J., Surový, P., … Kopecký, M. (2021).

576   Temperature buffering in temperate forests: Comparing microclimate models based on ground

577   measurements with active and passive remote sensing. *Remote Sensing of Environment*, *263*,

578   112522. https://doi.org/10.1016/j.rse.2021.112522

579 Kearney, M. R., & Porter, W. P. (2017). NicheMapR - an R package for biophysical modelling: the

580   microclimate model. *Ecography*, *40*(5), 664–674. https://doi.org/10.1111/ecog.02360

581 Kearney, M. R., Shamakhy, A., Tingley, R., Karoly, D. J., Hoffmann, A. A., Briggs, P. R., & Porter, W. P.

582   (2014). Microclimate modelling at macro scales: A test of a general microclimate model

583   integrated with gridded continental-scale soil and weather data. *Methods in Ecology and*

584   *Evolution*, *5*(3), 273–286. https://doi.org/10.1111/2041-210X.12148

585 Kopecký, M., Macek, M., & Wild, J. (2021). Topographic Wetness Index calculation guidelines based

586   on measured soil moisture and plant species composition. *Science of The Total Environment*,

587   *757*, 143785. https://doi.org/10.1016/j.scitotenv.2020.143785

588 Körner, C., & Hiltbrunner, E. (2018). The 90 ways to describe plant temperature. *Perspectives in Plant*

589   *Ecology, Evolution and Systematics*, *30*, 16–21. https://doi.org/10.1016/j.ppees.2017.04.004

590 Kuhn, M. (2012). The caret Package. *Journal of Statistical Software*, *28*.

591 Landuyt, D., Perring, M. P., Seidl, R., Taubert, F., Verbeeck, H., & Verheyen, K. (2018). Modelling

592   understorey dynamics in temperate forests under global change–Challenges and perspectives.

593   *Perspectives in Plant Ecology, Evolution and Systematics*, *31*, 44–54.

594   https://doi.org/10.1016/j.ppees.2018.01.002

595 Lembrechts, J. J., Aalto, J., Ashcroft, M. B., De Frenne, P., Kopecký, M., Lenoir, J., … Nijs, I. (2020).

596   SoilTemp: A global database of near-surface temperature. *Global Change Biology*, (March),

597   gcb.15123. https://doi.org/10.1111/gcb.15123

598 Lembrechts, J. J., & Lenoir, J. (2020). Microclimatic conditions anywhere at any time! *Global Change*

599   *Biology*, *26*(2), 337–339. https://doi.org/10.1111/gcb.14942

600   Lembrechts, J. J., Lenoir, J., Roth, N., Hattab, T., Milbau, A., Haider, S., … Nijs, I. (2019). Comparing

601   temperature data sources for use in species distribution models: From in-situ logging to remote

602   sensing. *Global Ecology and Biogeography*, (August 2018), geb.12974.

603   https://doi.org/10.1111/geb.12974

604   Lembrechts, J. J., Nijs, I., & Lenoir, J. (2018). Incorporating microclimate into species distribution

605   models. *Ecography*, 1–13. https://doi.org/10.1111/ecog.03947

606   Lenoir, J., Bertrand, R., Comte, L., Bourgeaud, L., Hattab, T., Murienne, J., & Grenouillet, G. (2020).

607   Species better track climate warming in the oceans than on land. *Nature Ecology & Evolution*,

608   *4*(8), 1044–1059. https://doi.org/10.1038/s41559-020-1198-2

609   Lenoir, J., Graae, B. J., Aarrestad, P. A., Alsos, I. G., Armbruster, W. S., Austrheim, G., … Svenning, J.-

610   C. (2013). Local temperatures inferred from plant communities suggest strong spatial buffering

611   of climate warming across Northern Europe. *Global Change Biology*, *19*(5), 1470–1481.

612   https://doi.org/10.1111/gcb.12129

613   Lenoir, J., Hattab, T., & Pierre, G. (2017). Climatic microrefugia under anthropogenic climate change:

614   implications for species redistribution. *Ecography*, *40*(2), 253–266.

615   https://doi.org/10.1111/ecog.02788

616   Lenoir, J., & Svenning, J.-C. (2013). Latitudinal and Elevational Range Shifts under Contemporary

617   Climate Change. In *Encyclopedia of Biodiversity* (pp. 599–611). https://doi.org/10.1016/B978-0-

618   12-384719-5.00375-0

619   Macek, M., Kopecký, M., & Wild, J. (2019). Maximum air temperature controlled by landscape

620   topography affects plant species composition in temperate forests. *Landscape Ecology*, *34*(11),

621   2541–2556. https://doi.org/10.1007/s10980-019-00903-x

622   Maclean, I. M. D. (2019). Predicting future climate at high spatial and temporal resolution. *Global*

623   *Change Biology*, (August), gcb.14876. https://doi.org/10.1111/gcb.14876

624   Maclean, I. M. D., Duffy, J. P., Haesen, S., Govaert, S., De Frenne, P., Vanneste, T., … Van Meerbeek,

625   K. (2021). On the measurement of microclimate. *Methods in Ecology and Evolution*, 2041-

626   210X.13627. https://doi.org/10.1111/2041-210X.13627

627   Maclean, I. M. D., Mosedale, J. R., & Bennie, J. J. (2019). Microclima: An <scp>r</scp> package for

628   modelling meso- and microclimate. *Methods in Ecology and Evolution*, *10*(2), 280–290.

629   https://doi.org/10.1111/2041-210X.13093

630   McLaughlin, B. C., Ackerly, D. D., Klos, P. Z., Natali, J., Dawson, T. E., & Thompson, S. E. (2017).

631   Hydrologic refugia, plants, and climate change. *Global Change Biology*, *23*(8), 2941–2961.

632   https://doi.org/10.1111/gcb.13629

633 Meeussen, C., Govaert, S., Vanneste, T., Haesen, S., Van Meerbeek, K., Bollmann, K., … De Frenne, P.
634   (2021). Drivers of carbon stocks in forest edges across Europe. *Science of The Total*
635   *Environment*, *759*, 143497. https://doi.org/10.1016/j.scitotenv.2020.143497

636 Meineri, E., Dahlberg, C. J., & Hylander, K. (2015). Using Gaussian Bayesian Networks to disentangle
637   direct and indirect associations between landscape physiography, environmental variables and
638   species distribution. *Ecological Modelling*, *313*, 127–136.
639   https://doi.org/10.1016/j.ecolmodel.2015.06.028

640 Meineri, E., & Hylander, K. (2017). Fine-grain, large-domain climate models based on climate station
641   and comprehensive topographic information improve microrefugia detection. *Ecography*,
642   *40*(8), 1003–1013. https://doi.org/10.1111/ecog.02494

643 Monin, A. S., & Obukhov, A. M. (1954). Basic laws of turbulent mixing in the surface layer of the
644   atmosphere. *Contrib. Geophys. Inst. Acad. Sci. USSR*, *151(163)*, e187.

645 Muñoz-Sabater, J., Dutra, E., Agust\'\i-Panareda, A., Albergel, C., Arduini, G., Balsamo, G., … Thépaut,
646   J.-N. (2021). ERA5-Land: A state-of-the-art global reanalysis dataset for land applications. *Earth*
647   *System Science Data Discussions*, *2021*, 1–50. https://doi.org/10.5194/essd-2021-82

648 Niittynen, P., & Luoto, M. (2018). The importance of snow in species distribution models of arctic
649   vegetation. *Ecography*, *41*(6), 1024–1037. https://doi.org/10.1111/ecog.03348

650 Nilsson, M. C., & Wardle, D. A. (2005). Understory vegetation as a forest ecosystem driver: Evidence
651   from the northern Swedish boreal forest. *Frontiers in Ecology and the Environment*, *3*(8), 421–
652   428. https://doi.org/10.1890/1540-9295(2005)003[0421:UVAAFE]2.0.CO;2

653 Pacifici, M., Foden, W. B., Visconti, P., Watson, J. E. M., Butchart, S. H. M., Kovacs, K. M., … Rondinini,
654   C. (2015). Assessing species vulnerability to climate change. *Nature Climate Change*, *5*(3), 215–
655   224. https://doi.org/10.1038/nclimate2448

656 Pecl, G. T., Araújo, M. B., Bell, J. D., Blanchard, J., Bonebrake, T. C., Chen, I.-C., … Williams, S. E.
657   (2017). Biodiversity redistribution under climate change: Impacts on ecosystems and human
658   well-being. *Science*, *355*(6332), eaai9214. https://doi.org/10.1126/science.aai9214

659 Perry, D. A. (1994). *Forest Ecosystems*. Johns Hopkins University Press.

660 Pincebourde, S., & Woods, H. A. (2020). There is plenty of room at the bottom: microclimates drive
661   insect vulnerability to climate change. *Current Opinion in Insect Science*, *41*, 63–70.
662   https://doi.org/10.1016/j.cois.2020.07.001

663 Potter, K. A., Arthur Woods, H., & Pincebourde, S. (2013). Microclimatic challenges in global change
664   biology. *Global Change Biology*, *19*(10), 2932–2939. https://doi.org/10.1111/gcb.12257

665 R Core Team. (2020). *R: A Language and Environment for Statistical Computing*. Vienna, Austria.

666 Richardson, L. F. (1922). Weather prediction by numerical process. *Cambridge UK: Cambridge*

667   *University Press*.

668   Ridgeway, G. (2005). *Generalized boosted models: A guide to the gbm package*.

669   Roberts, D. R., Bahn, V., Ciuti, S., Boyce, M. S., Elith, J., Guillera-Arroita, G., … Dormann, C. F. (2017).

670   Cross-validation strategies for data with temporal, spatial, hierarchical, or phylogenetic

671   structure. *Ecography*, *40*(8), 913–929. https://doi.org/10.1111/ecog.02881

672   Scheffers, B. R., De Meester, L., Bridge, T. C. L., Hoffmann, A. A., Pandolfi, J. M., Corlett, R. T., …

673   Watson, J. E. M. (2016). The broad footprint of climate change from genes to biomes to people.

674   *Science*, *354*(6313), aaf7671. https://doi.org/10.1126/science.aaf7671

675   Senf, C., & Seidl, R. (2021). Mapping the forest disturbance regimes of Europe. *Nature Sustainability*,

676   *4*(1), 63–70. https://doi.org/10.1038/s41893-020-00609-y

677   van den Hoogen, J., Geisen, S., Routh, D., Ferris, H., Traunspurger, W., Wardle, D. A., … Crowther, T.

678   W. (2019). Soil nematode abundance and functional group composition at a global scale.

679   *Nature*, *572*(7768), 194–198. https://doi.org/10.1038/s41586-019-1418-6

680   van den Hoogen, J., Robmann, N., Routh, D., Lauber, T., van Tiel, N., Danylo, O., & Crowther, T. W.

681   (2021). A geospatial mapping pipeline for ecologists. *BioRxiv*, 1–9.

682   https://doi.org/10.1101/2021.07.07.451145

683   Vercauteren, N., Destouni, G., Dahlberg, C. J., & Hylander, K. (2013). Fine-Resolved, Near-Coastal

684   Spatiotemporal Variation of Temperature in Response to Insolation. *Journal of Applied*

685   *Meteorology and Climatology*, *52*(5), 1208–1220. https://doi.org/10.1175/JAMC-D-12-0115.1

686   Willis, K. J., & Bhagwat, S. A. (2009). Biodiversity and Climate Change. *Science*, *326*(5954), 806–807.

687   https://doi.org/10.1126/science.1178838

688   Wilson, A. M., & Jetz, W. (2016). Remotely Sensed High-Resolution Global Cloud Dynamics for

689   Predicting Ecosystem and Biodiversity Distributions. *PLOS Biology*, *14*(3), e1002415.

690   https://doi.org/10.1371/journal.pbio.1002415

691   Zellweger, F., Coomes, D., Lenoir, J., Depauw, L., Maes, S. L., Wulf, M., … De Frenne, P. (2019).

692   Seasonal drivers of understorey temperature buffering in temperate deciduous forests across

693   Europe. *Global Ecology and Biogeography*, *28*(12), 1774–1786.

694   https://doi.org/10.1111/geb.12991

695